Electronic Supplementary Material (ESI) for Journal of Materials Chemistry A.

Supporting Information

Electrochromic and energy storage bifunctional Gd-doped WO_3/Ag/WO_3 films

Yi Yin, Tian Gao, Qingfan Xu, Gangqiang Cao, Qi Chen, Haoyu Zhu, Changyong Lan, Chun Li**

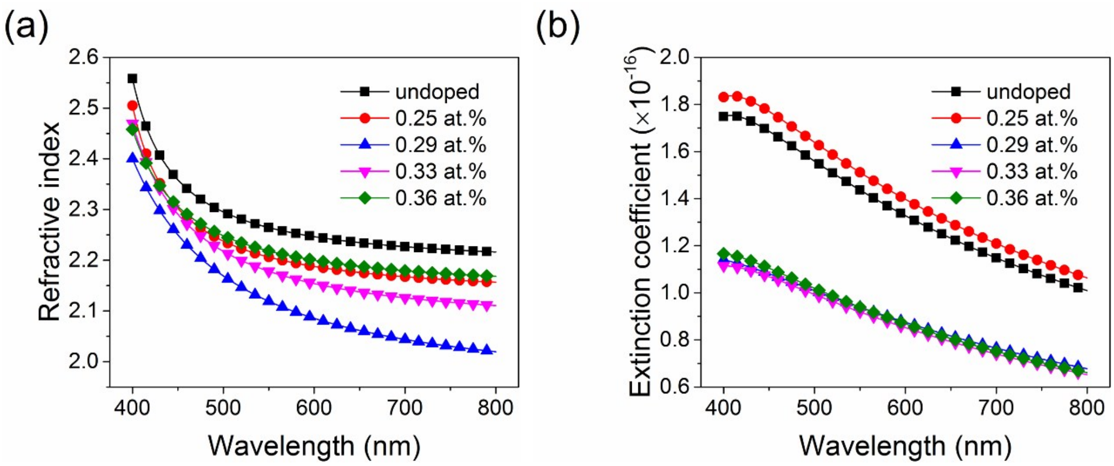

Figure S1. Measured (a) refractive indices *n* and (b) extinction coefficient *k* of sputtering WO_3 films on glass substrate with various Gd doping levels.

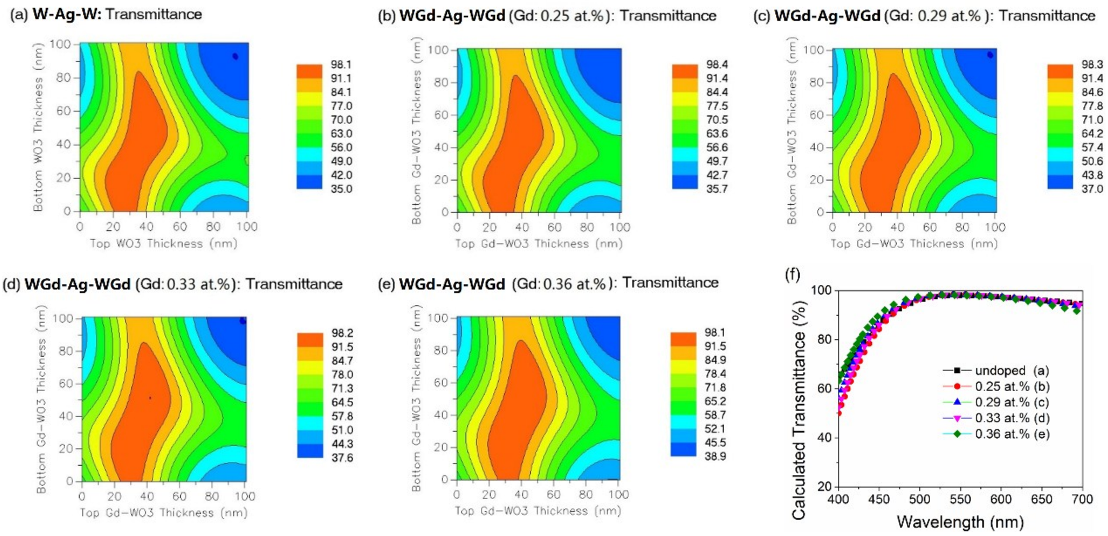

Figure S2. Calculated (a)-(e) contour plots of transmittance (λ =550 nm) and (f) transmittance spectra for WGd-Ag-WGd structures upon variation of the thickness of Top-and-Bottom WGd layers (0～0.36 at% Gd-doped).

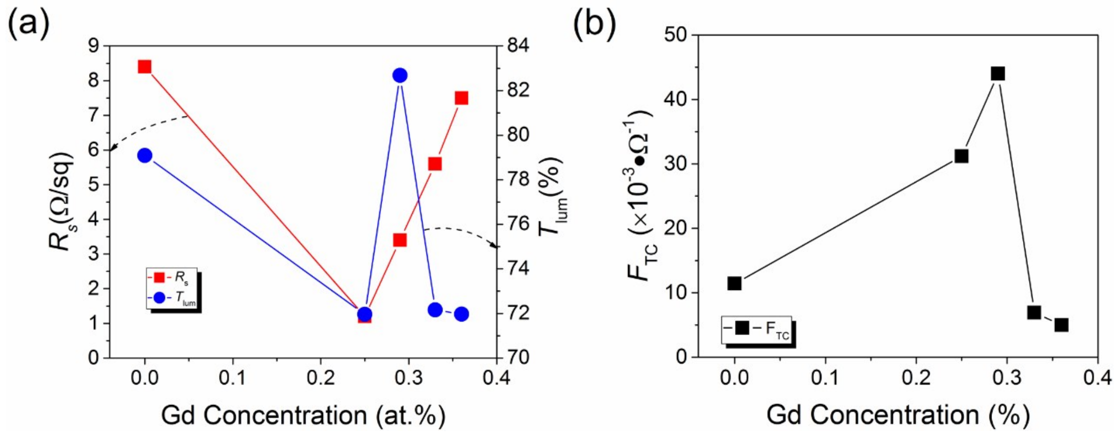

Figure S3. (a) Calculated luminous Transmittance (T_{lum}) and actual tested sheet resistance (R_{s}), (b) Calculated Figure-of-Merit (F_{TC}) results for WGd-Ag-WGd Films with different Gd doped content

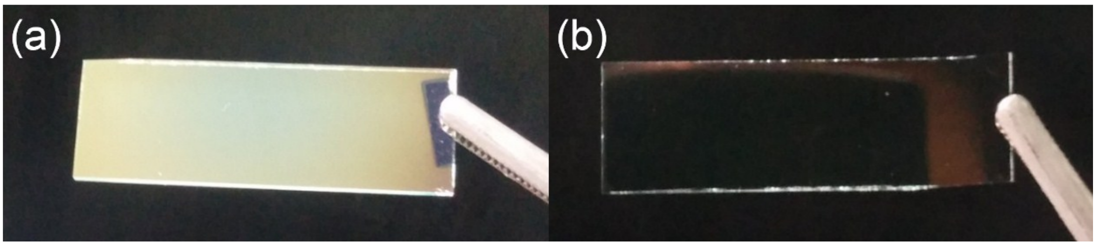

Figure S4. Photographs of the typical WGd-Ag-WGd samples (a) without and (b) with a sacrificial Gd-WO_x layer, which clearly show an optically hazy and clear appearance, respectively.

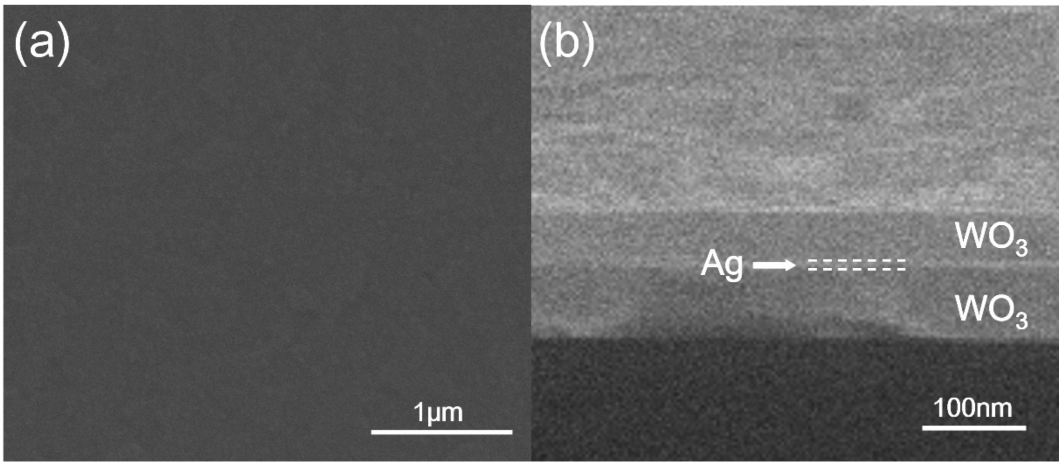

Figure S5. SEM images of (a) surface and (b) cross-sectional microstructures of the W-Ag-W films

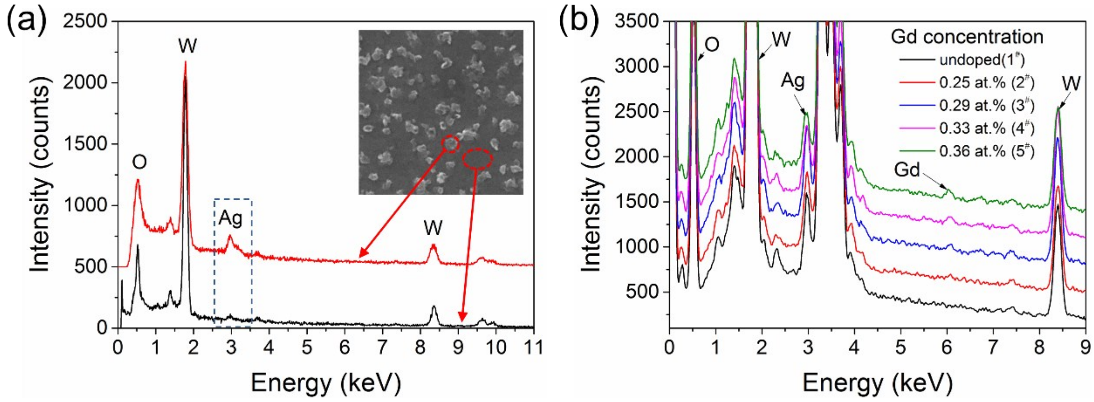

Figure S6. Surface EDS patterns of (a) WGd-Ag-WGd film without a pre-deposited Gd-WO_x layer* and (b) WGd-Ag-WGd film on glass substrates with varying Gd concentration. The samples of (b) were numbered from $1^{\#}$ to $5^{\#}$ and the corresponding thicknesses of each layer are listed in Table S1.

*Figure S9a shows that the Ag content of the clusters on surface is obviously higher than that of non-agglomerates regions. The WGd-Ag-WGd film without a pre-deposited Gd-WO_x layer is just used to see if protection against silver oxidation is successful. Poor conductivity prevents it from being used as an electrochemical electrode material and thus it is not the research focus in this paper.

Table S1 EDS analysis of the chemical compositions for WGd-Ag-WGd Films with different Gd doped content

Sample No	Thicknesses(nm) WGd-Ag-WGd	Gd (at.%)	W (at.%)	Ag (at.%)	O (at.%)	Gd/W ratio
1	51-12-41	-0.02	14.71	2.25	83.06	——
2	52-12-41	0.25	14.35	2.28	83.12	0.0174
3	52-12-42	0.29	14.33	1.63	83.75	0.0202
4	51-12-42	0.33	14.44	1.89	83.34	0.0229
5	50-12-42	0.36	13.76	1.10	84.78	0.0262

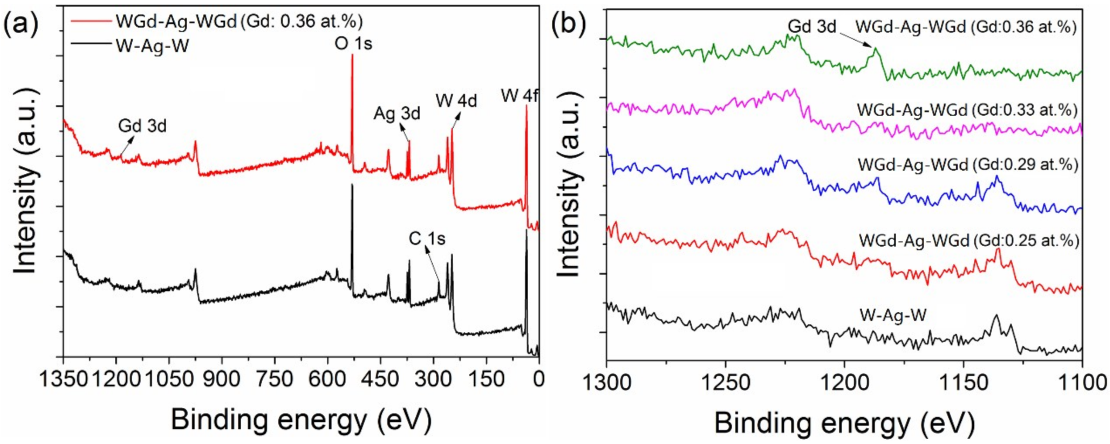

Figure S7. (a) Full spectra of XPS survey scanning of W-Ag-W and WGd-Ag-WGd (Gd: 0.36 at.%) films on glass; (b) Intensity of Gd 3d characteristic peak strengthens with increasing of doping concentration from 0 to 0.36 at.%.

Peak area sensitivity factors methods.

To determine the relative concentrations (C_X) of the various constituents in these WO_3 samples, peak area sensitivity factors methods were used in this paper (The binding energies and peak area for all the peaks are calculated and the corresponding sensitivity factors are listed in Table S1 by consulting the XPS operations manuals.).

A generalized expression can be written as:

$$C_X = \frac{I_X / S_X}{\sum_i I_i / S_i},$$

where I_x is the peak area of required elements, S_x is the corresponding required atomic sensitivity factor, I_i is the peak area of i-th trace elements, and S_i is the corresponding i-th atomic sensitivity factor.

Table S2. XPS data of W 4*f*, Ag 3*d*, Gd 3*d* and O 1*s* for W-Ag-W and WGd-Ag-WGd (Gd:0.25～0.36 at.%) films

Sample No		W^{+6} $4f_{7/2}$	Ag^{+} $3d_{5/2}$	Gd^{3+} $3d_{5/2}$	O^{-2} $1s$
	Sensitivity factor	2.0	2.25	29.4	0.63
1	Binding energy(eV)	35.57	368.23	——	530.49
	Peak area	59187.30	34981.09	——	56352.38
2	Binding energy(eV)	35.52	368.16	1187.58	530.47
	Peak area	49024.76	53531.04	12734.25	46083.91
3	Binding energy(eV)	35.52	368.11	1187.38	530.37
	Peak area	58693.75	9646.63	17327.2	54035.27
4	Binding energy(eV)	35.43	368.08	1187.28	530.33
	Peak area	60153.40	5837.16	20241.76	54105.44
5	Binding energy(eV)	35.26	367.90	1187.18	530.22
	Peak area	57014.55	67678.68	22463.34	50371.88

Table S3 XPS analysis of the chemical compositions for WGd-Ag-WGd Films with different Gd doped content

Sample No	Thicknesses(nm) WGd-Ag-WGd	Gd/W ratio	O/W ratio
1	51-12-41	——	3.0225
2	52-12-41	0.0177	2.9842
3	52-12-42	0.0201	2.9226
4	51-12-42	0.0229	2.8554
5	50-12-42	0.0268	2.8047

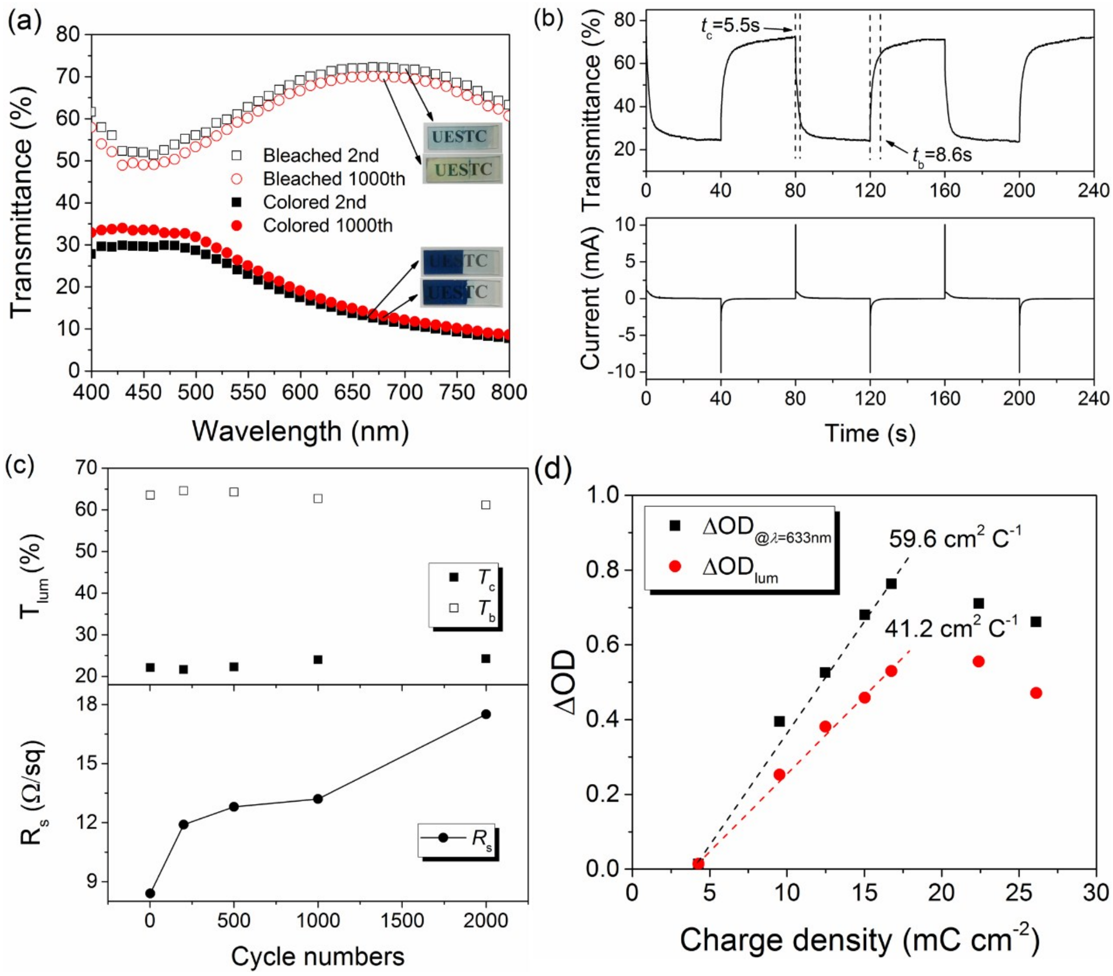

Figure S8. (a) Optical transmittance spectra of the colored and bleached states after the 2nd and the 2000th CV cycling of the optimized W-Ag-W sample. Inset shows the corresponding optical images of bleached (top) and colored (bottom) states after the 2000th cycling. (b) Corresponding in situ transmittance curves (top half) at 633nm wavelength to CA (bottom half). (c) Monitored variation of luminous transmittance T_{lum} and sheet resistance R_s curves during 2000 potential step cycles (from +1 to -1 V vs. Ag/AgCl) of the WAW film. Inset shows the corresponding cyclic voltammetry (CV) curves. (d) Optical density calculated with transmittance at 633 nm and luminous transmittance of W-Ag-W film, respectively, as a function of charge density.

The methods for calculating areal capacitance from Cyclic voltammetry (CV) cycling curves

The areal capacitance (Ca, mF cm^{-2}) is calculated according to the following formula (**Supporting Info,** ***Angew. Chem. Int. Ed***. **2014, 53, 11935-11939**):

$$C_a = \frac{Q}{A\Delta V}$$

where Q represents the injected charge, A represents the active area of electrode, and ΔV represents the potential window. For CV curves, the Q can be calculated according to the following formula (**Supporting Info,** ***Angew. Chem. Int. Ed***. **2014, 53, 11935-11939**):

$$Q = \int_0^t idt = \frac{1}{2v}\int_0^t idU = \frac{S}{2v}$$

where S represents the loop areas of CV curves, v represents the scan rate.

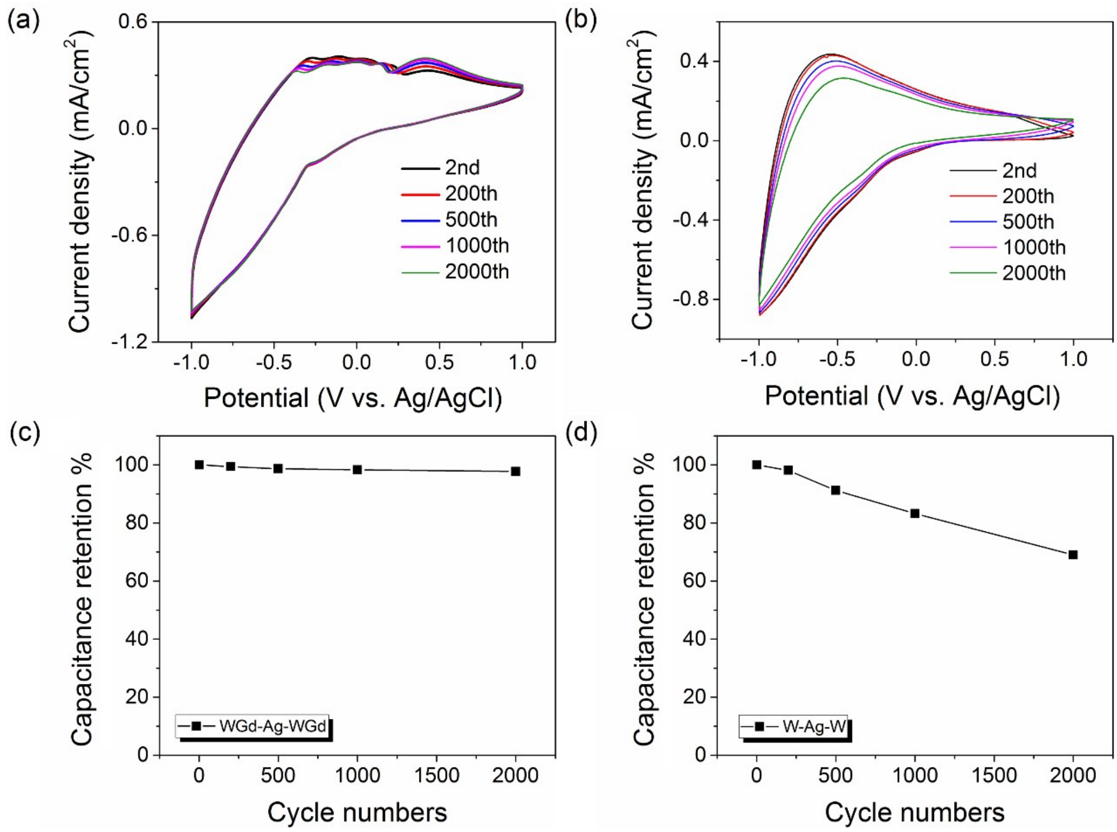

Figure S9. Cyclic voltammetry (CV) cycling stability of (a) WGd-Ag-WGd and (b) W-Ag-W films measured at a scan rate of 50 mV s^{-1} for 2000 cycles. Long-term capacitance stability curve of (c) WGd-Ag-WGd and (d) W-Ag-W films obtained through CV cycling testing.

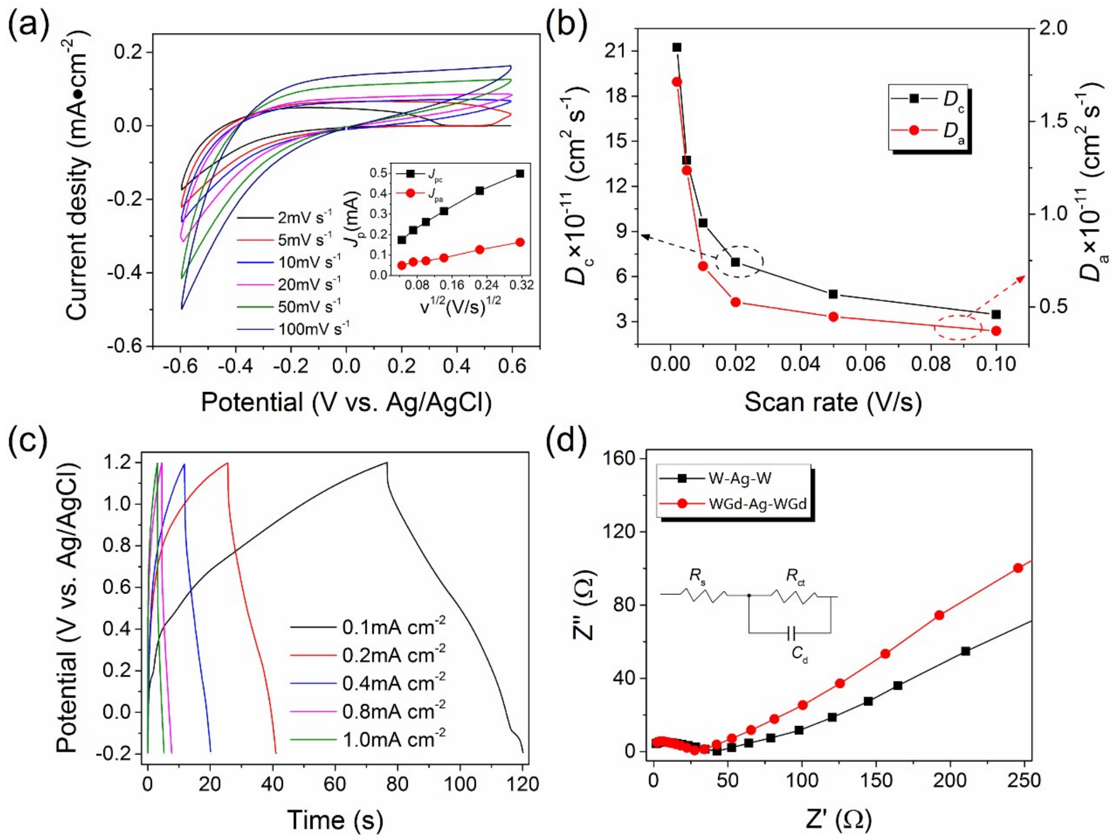

Figure S10. (a) CV curves of optimized W-Ag-W film on glass substrate at different scan rates. Inset shows the cathodic and anodic peak current densities (J_{pc} and J_{pa}) as a function of square root of scan rate $v^{1/2}$ tested at room temperature, respectively. (b)Variation curve of diffusion coefficient (D_a and D_c) corresponding to cathodic and anodic current densities with scan rate v, respectively. (c) Galvanostatic charging and discharging curves of W-Ag-W film at different current density. (d) Nyquist plots of W-Ag-W and WGd-Ag-WGd films on glass after the 2000th CV cycling. Insets are their fitted equivalent circuit.